Aust. J. Phys., 1974, **27**, 401–10

A Determination of the Daytime Thermospheric Wind Profile by Observing a Lithium Trail with a Field-of-view Scanner

A. D. Hind and K. H. Lloyd

Weapons Research Establishment, P.O. Box 2151, Adelaide, S.A. 5001.

Abstract

A description is given of the design of an instrument which has been built to detect the lithium 671 nm line against the daytime sky continuum. The instrument covers the field of view by means of a servo-controlled scanning mirror and detects the lithium line by chopping the received beam and using phase sensitive detection. Data obtained for a daytime release of lithium between 90 and 130 km altitude are presented, and the methods for the analysis of these data to obtain a wind profile of the upper atmosphere are described. The derived wind profile is similar in its main features to those observed at twilight and night.

Introduction

The release of chemical tracers from rockets into the upper atmosphere has proved to be a powerful tool for the determination of transport processes over the altitude range 80–200 km. The technique, which has been in use for nearly 15 years, consists of observing the vapour release at twilight by means of resonant scattering of the incident solar radiation against a dark sky foreground (Manring *et al.* 1959) or at night by means of a chemiluminescent reaction between the chemical tracer and the ambient atmosphere (Rosenberg and Golomb 1963). The confinement of the observation period to less than half of the day has meant that study of the propagation of tides in the atmosphere is necessarily incomplete (Murphy and Bull 1968). Alternatively bold assumptions must be made to determine the magnitude of these tides (Woodrum and Justus 1968).

Recently, Bedinger (1970), Best (1970) and Rees *et al.* (1972) have described various techniques, based on narrow pass band interference filters, which are able to detect lithium against the sky foreground in daytime. However, the detection of lithium is only part of the problem, since the determination of the wind profile of the upper atmosphere from the observed data also presents many difficulties. The problem of triangulation must evidently exist also for the technique of observing lithium trails from aircraft, as Bedinger (1973) did not present any wind profile from the trail which he observed.

On 21 June 1973, two hours after sunrise, a trail of lithium released from a rocket was observed at Woomera (136° E., 31° S.) by means of two ground-based detectors built for the purpose. This paper reports the thermospheric wind profile determined from these observations. Since our equipment employed several techniques not yet reported in the literature, and since the data analysis necessitated the development of

methods which were basically different from conventional photogrammetry, we have included a description of both. The instrument and the analysis techniques are discussed in greater detail by Hind and Lloyd (1973).

Description of Instrument

The principle of operation of the detector is similar to that of the detectors described by Bedinger (1970) and Best (1970), in which light from the sky is chopped mechanically so that alternate beams pass normally, and at incidence, through a narrow pass band filter centred on the lithium 670·7 nm line. The difference signal between the two beams gives the intensity of light in the lithium line.

A photograph of the instrument is given in Fig. 1*a*, and schematic diagrams of its optical construction and electronic components are given in Figs 1*b* and 1*c* respectively. The light from the lithium cloud and the foreground sky are reflected by the plane mirror through the 75 mm diameter 620 mm focal length convex lens, which focuses the image on the field-of-view stop. The stop consists of a disc with a series of holes on its circumference, enabling an angular resolution of between 0·02° and 0·3° to be chosen. Behind the field-of-view stop lies a chopper disc with four pairs of reflecting and transparent sectors. The chopper disc is rotated by a d.c. motor to provide a chopping frequency of 300 Hz. When the transparent sectors are in the optical path, the beam passes directly through to the field lens, which is focused on the aperture stop, and then through the interference filter on to the cathode of the photomultiplier. The reflecting sectors of the chopper disc reflect the beam down into the prism, whence by total internal reflection it passes up through the field lens and interference filter at an angle of 3° to the optic axis (i.e. 0·3 nm off the pass band maximum). The optical path length of the beam in the prism has been designed so that the entrance aperture is also focused onto the photocathode. The reflecting prism is mounted on a cradle pinioned on two orthogonal axes, and is adjusted so that the images of the direct and reflected beams are superposed on the photocathode. The interference filter is mounted in front of the photomultiplier inside a standard Peltier cooling chamber, so that the filter temperature can be held constant. A slot cut in the side of the cooling chamber allows the suitably mounted filter to be removed for performing star calibrations (see next section).

The cooling chamber is mounted on a cradle, which can move along the optic axis of the instrument for adjustment of focus. It can also be swivelled about the two axes normal to the optic axis to allow for adjustment of the angle of incidence of the beam on the interference filter. We have chosen the direct beam to be that for which the angle of incidence is such that the lithium line is transmitted. This was achieved by illuminating the instrument with light from a lithium lamp, and adjusting the angular position of the cooling chamber until the d.c. signal from the photo-

Fig. 1 (*opposite*). Instrument for detecting a lithium trail against the sky foreground in the daytime:
(*a*) Photograph of the instrument; A marks the removable lithium lamp used for calibration.
(*b*) Schematic diagram of the detector optics. The abbreviations used are: SM, scanning mirror; OL, object lens (*f*/8) of 620 mm focal length; FS, field-of-view stop; CD, chopper disc (the alternating transmitting T and reflecting R segments are indicated in the front-on view shown directly above); TP, total internal reflection prism; KE, knife edge; FL, field lens (*f*/4) of 140 mm focal length; IF, interference filter (0·3 nm pass band); PT, photomultiplier tube; CC, cooling chamber.
(*c*) Block diagram of the electronics.

(*a*) Instrument

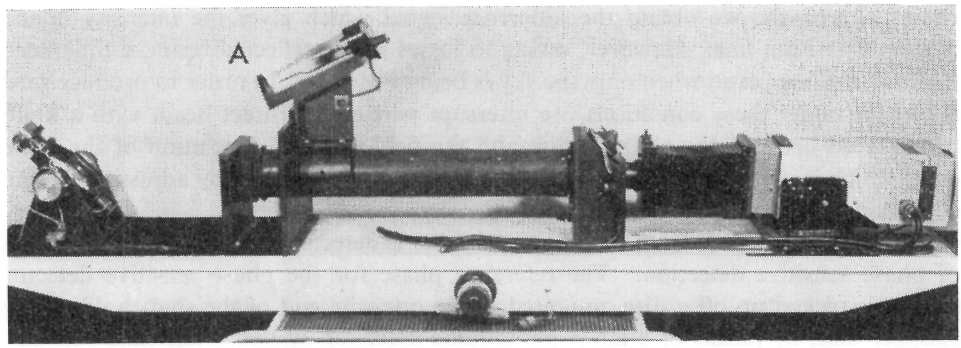

(*b*) Optics

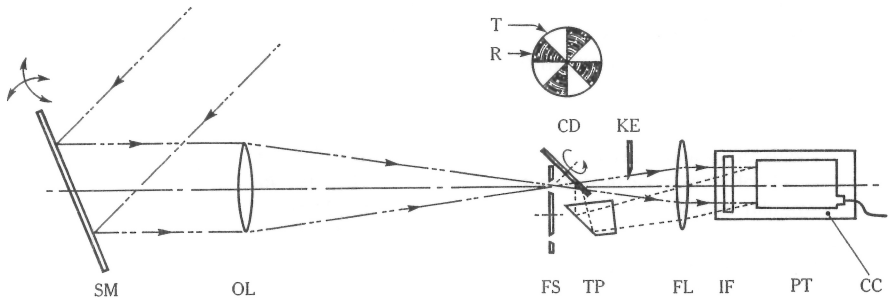

(*c*) Electronics

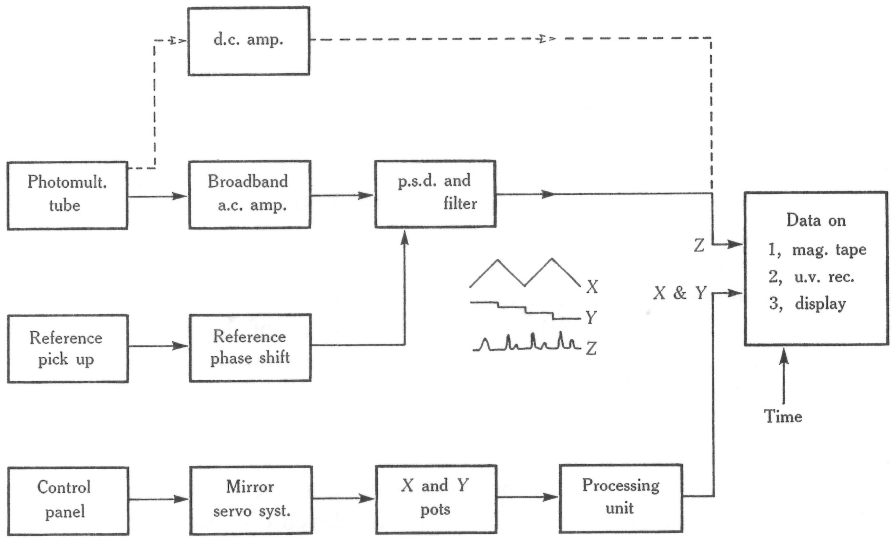

multiplier was a maximum. With the chamber in this position, the rays which are reflected via the prism now strike the interference filter at an angle such that the pass band is shifted 0·3 nm from the lithium line. This means that by detecting the signal from the direct (lithium plus foreground sky) and reflected (foreground sky only) beams alternately, we obtain the difference signal which gives the intensity in the lithium 670·7 nm line. However, owing to losses in the reflected beam, a difference signal is obtained even when only the sky is being observed. In order to produce zero difference under these conditions, we interrupt part of the direct beam with a knife edge placed between the chopper disc and the field lens. The position of the knife edge, which is adjusted by a screw, is set shortly before the firing by adjusting for the condition of zero output when scanning the sky.

The difference signal from the photomultiplier is detected by the standard methods of phase sensitive detection. The reference phase for the phase sensitive detector (p.s.d.) is picked up off a disc, mounted at the opposite end of the shaft holding the chopper disc, by means of a lamp–photodiode detection system. The time constant of the p.s.d. has to effect a compromise between the requirements of a narrow pass band to maintain a good signal to noise ratio and of a fast response to a changing signal. Provision has been built into the control electronics for varying the fields of view, scan times and number of scan lines, all of which have to be considered when setting the time constant. A summary of the operating parameters and the available settings, with the most commonly used settings given in italics, is as follows:

Fields of view in horizontal direction	20°, 40°, *50°*
Fields of view in vertical direction	20°, 30°, *40°*
Angular resolutions	0·02°, 0·05°, 0·1°, 0·2°, *0·3°*
Numbers of scan lines in a frame	8, 16, *32*, *64*, 128
Times to scan one line	1, *2*, 4, 8 s
Frequency at which beam is chopped	300 Hz
Time constants of p.s.d.	1 ms to 10 s in 9 steps (*3* ms)

These parameters are selected on a remote console which also houses the display screens, the data recorders and other ancillary equipment.

As mentioned in the Introduction, the detection of the signal is only half of the problem, the determination of the azimuth and elevation of the object being just as important. The optical components of the instrument are mounted on a 150 × 30 cm aluminium base, with a webbed structure underneath to provide strength without weight. The base, which defines the optic axis of the instrument, is mounted on a rotatable mount with calibrated scales, so that the optic axis of the instrument can be set to any required azimuth and elevation.

The scanning mirror is driven by two servo motors. By driving the motor on the X axis with a triangular voltage, and that on the Y axis with a staircase voltage, the mirror is made to scan a rectangular raster. The position of the mirror is determined by pick-up from the two feedback potentiometers. The accuracy of the measurement of azimuth and elevation is therefore determined by the stability of this voltage source and of the drift in the system. These parameters are checked by recording the potentiometer supply voltages at the beginning and end of each frame.

The voltages from the X and Y potentiometers and the output of the p.s.d. are recorded on magnetic tape. The output is also displayed on a storage display screen to facilitate the choice of optimum control settings. The field of view is varied to keep

the lithium trail in view and to avoid wasting information by scanning only the sky. During observations, the scan speed and p.s.d. time constant are altered to optimize the information from the initial sharp-edged dense cloud to the later diffuse cloud. Examples of the display at different times are shown in Fig. 2. These were photographed on an additional display by means of a 35 mm camera.

Prior to making star angular calibrations, the interference filter is removed from the cooling chamber and the temperature of the latter is set at its minimum value to reduce the photomultiplier dark current. The phase sensitive detection facility is then used to detect the star, the difference signal being produced by winding in the knife edge so that the direct beam is totally interrupted. For Sun or Moon calibrations, which are only performed if it is not possible to do star calibrations, the interference filter is left in place and an additional neutral density filter placed in the entrance aperture.

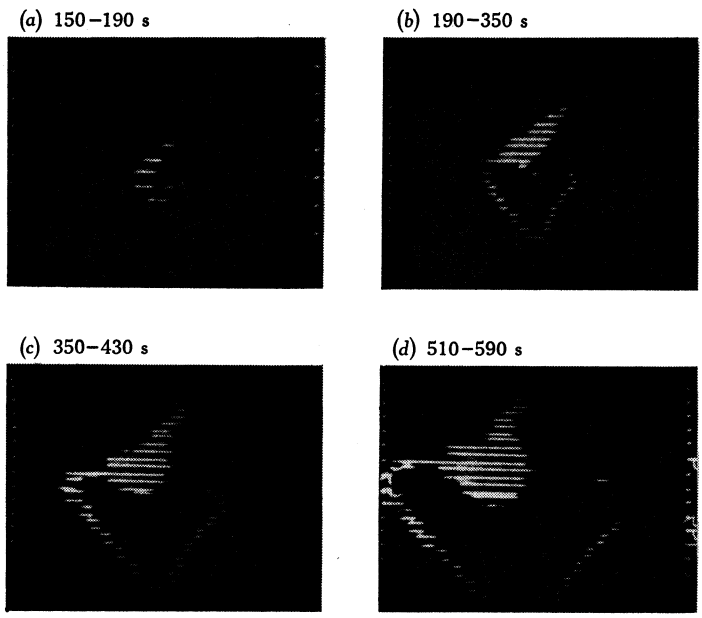

Fig. 2. Montage of 35 mm photographs taken of the cathode ray oscilloscope display of the lithium trail at the indicated times. All frames show a 50° × 40° field of view, and dots at the sides of each frame are end-of-scan markers.

The star calibrations are made with the mount in the same setting as for the trail observations, thereby eliminating any errors in the mount calibrations. This is not possible for Sun or Moon calibrations, and in order to calibrate the whole field of view it is necessary to make several calibrations with the scanner mount at different angular settings.

Angular Calibration of Line of Sight

As is done for photogrammetry, we have chosen to calibrate the instrument by observing stars (or Sun or Moon) at known times, rather than attempt to determine the lines of sight of the data directly. However, because of the reflection in the scanning mirror, the field of view is strongly off axis, and the photogrammetric method of

using standard coordinates is not applicable. The absolute azimuth and elevation of the mount are required for the calibrations and, provided that these are correct to within 1°, a least squares fitting technique may be used to supply the necessary correction. Note, however, that accurate ($\sim 0{\cdot}1°$) relative positions of the scanner mount are required.

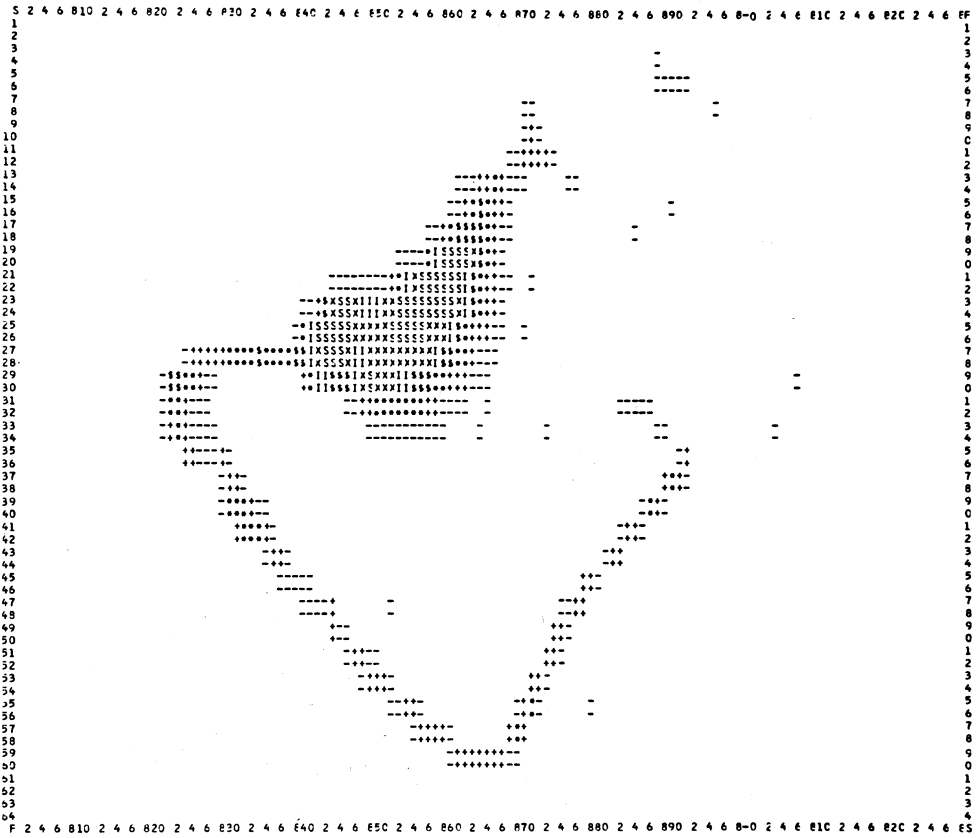

Fig. 3. Computer plotted isophotes of the lithium release obtained from the magnetic tape data for the firing of 21 June 1973. This matrix should be compared with the frame shown in Fig. 2*c*.

The calibration data consist of a series of scanner mirror potentiometer voltages (V_x, V_y) for the observed positions of the stars (or Sun or Moon), together with the corresponding azimuth and elevation of the optic axis (given by the scanner mount scale readings (A,E)). The computed true azimuth and elevation of each star is then converted to azimuth and elevation with respect to the scanner optic axis (A_s, E_s) from the known values of A and E by means of the relation for the equality of the angles of incidence and reflection in the scanner mirror. Since the potentiometers are linear, their output is proportional to angle, and we can use a linear least squares fit of the voltage data onto the calculated angles (A_s, E_s). The best fit coefficients determined from the least squares analysis are then used to convert the potentiometer voltage data of the lithium trail to angles with respect to the optic axis, and hence to true azimuth and elevation.

Analysis of Data on Lithium Trail

The magnetic tape data on the lithium trail are fed into a computer, which reconstructs, frame by frame, the isophotes of the trail. Fig. 3 shows one such computer-plotted isophote, which should be compared with the frame shown in Fig. 2*c*. The computer also punches out a deck of data cards, one card for each matrix point whose radiance is above the background. The deck is edited to contain only the locus of the centre of the trail, and the potentiometer voltages of the corresponding points are then converted to true azimuth and elevation.

Since the data are obtained by scanning down the field of view, it is not possible to compute the locus of the trail in space by methods of photogrammetry in which the trail at a given instant of time is photographed from two sites. Other methods must be used to analyse the data. We have developed two methods for analysing the time sequenced data from two sites, one rigorously mathematical and the other intuitive. These are outlined in turn.

The data consist of a set of observations from the two sites of the form (A_T, E_T, t), A_T and E_T being the true azimuth and elevation of an observed point at time t. The problem of calculating the wind profile from these data can be stated mathematically as that of finding a function (the wind profile) which minimizes a defined error criterion (the sum of the squared differences between the observations and the function). In order to develop this mathematical technique, it is necessary to define the velocity profile in functional form, and we have chosen to expand the northward and westward wind components each in a Chebyshev series

$$V(\theta) = \sum_{n=1}^{N} A_n T_n(\theta), \qquad \text{with} \qquad \theta = (h-h_0)/(h_{\max}-h_{\min}),$$

where the T_n are Chebyshev polynominals, the A_n are the series coefficients, θ is a normalized altitude, and h_0 is the mean of $h_{\max}$ and $h_{\min}$. The values of h_0, $h_{\max}$ and $h_{\min}$ are chosen so that $-1 \lesssim \theta \lesssim 1$ over the range of altitudes spanned by the trail.

The error parameter we have adopted is the square of the angle between the observation and the calculated position of the trail for the assumed wind profile. The procedure is now described. A set of values for the A_n is chosen and the corresponding wind profile is calculated. For the time of each datum point, the position of the trail at each of a set of chosen altitudes is calculated (we also need to know the release position of the trail from radar trajectory data). The angle between the observed direction of the datum point and each of the computed directions along the trail is then calculated, and the minimum value of this angle is taken as the error for that datum point. The altitude of the closest computed direction should lie close to the altitude of the observed element of the trail.

The problem is to choose expansion coefficients for the wind profile which minimize the sum of the squares of the angular differences. Such minimization problems are well-defined mathematically, and a variety of procedures have been developed to solve them. The one which seems most suitable for our purpose is the algorithm developed by Powell (1964), which finds the minimum by searching in function space along a series of conjugate directions generated by the searching technique. The method has the additional advantage of not requiring the calculation of derivatives of the error with respect to the expansion coefficients.

As with all minimization procedures, it is necessary to provide the routine with a first estimate for the wind profile. It is important that this be close to the true profile, for otherwise the search procedure may find a local minimum, and not the true absolute minimum. We now describe two empirical methods for determining the wind profile, which can also be used for the first estimate in the mathematical technique.

The first method consists of interpolating the trail loci (Fig. 2), in which time increases down the frame, to obtain loci at given instants of time. These can then be analysed as for photogrammetry, but they suffer from the difficulty of identifying corresponding points between which one must interpolate. However, for a profile with well-defined kinks, such as that reported in this paper, the problem is eased.

The second method consists of identifying corresponding points on two frames from both sites (such as the ends of the trail, breaks in the trail, kinks etc.). For each site, these data define a plane along which the line of drift of the identified point lies, and the intersection of two such planes from the two sites defines the line of drift. Since the drift is predominantly horizontal (an assumption we make throughout our analysis) the departure of the line obtained by this method from the horizontal gives an indication of the accuracy of the method.

Results

On 21 June 1973 at 0850 h C.S.T. (2 hours after local sunrise) the first observations were made of a lithium release under full daylight conditions by our instrument. The trail was released by a Cockatoo sounding rocket, launched from Woomera. The trail was observed by the instrument for over 30 min, but little useful data were obtained after 15 min because much of the trail had drifted out of the field of view. The montage shown in Fig. 2 was made from photographs of the c.r.o. display of the scanned trail.

The final wind profile obtained from the data analysis is shown in Fig. 4. Because the site from which the data in Figs 2 and 3 were taken lay directly underneath the release of the trail, the subsequent shape of the trail corresponded closely to the wind profile. Although this meant that an extremely accurate estimate of the wind at the various points could be obtained, it made it very difficult to determine the altitude of the points. The solid curve in Fig. 4 was obtained from the data interpolated to given times. Its shape corresponds in detail to the observed locus of the cloud (Fig. 2), as obtained with the scanner located beneath the cloud. The open circles are results obtained from the identifiable kinks on the observed locus. We have averaged the results derived by means of the points from the several frames in various combinations. The indicated altitudes were then obtained by combining the results from the interpolated time and the identified points data, and are accurate to ± 4 km.

The dashed curve in Fig. 4 was obtained by applying Powell's method to the minimization of the error between the observed data and the profile being tested. Because it was obtained from the actual data, the dashed profile is more accurate in its gross features than the solid profile. This is especially true for the altitude assignments, which are accurate to ± 2 km. An indication of this accuracy is given by comparing the altitudes at which the prescribed wind profile gave the closest fit to the identifiable kinks in the trail. It is surprising how much more consistent these altitudes are than those obtained by the method of triangulating on the identifiable kinks. The poly-

nomial expansion method has the disadvantage that it is unable to follow the small structure of the wind profile. The dashed profile plotted in Fig. 4 used an eighth-order Chebyshev polynomial expansion in each of the velocity components; to have used a greater number of coefficients would have been prohibitive in computer time.

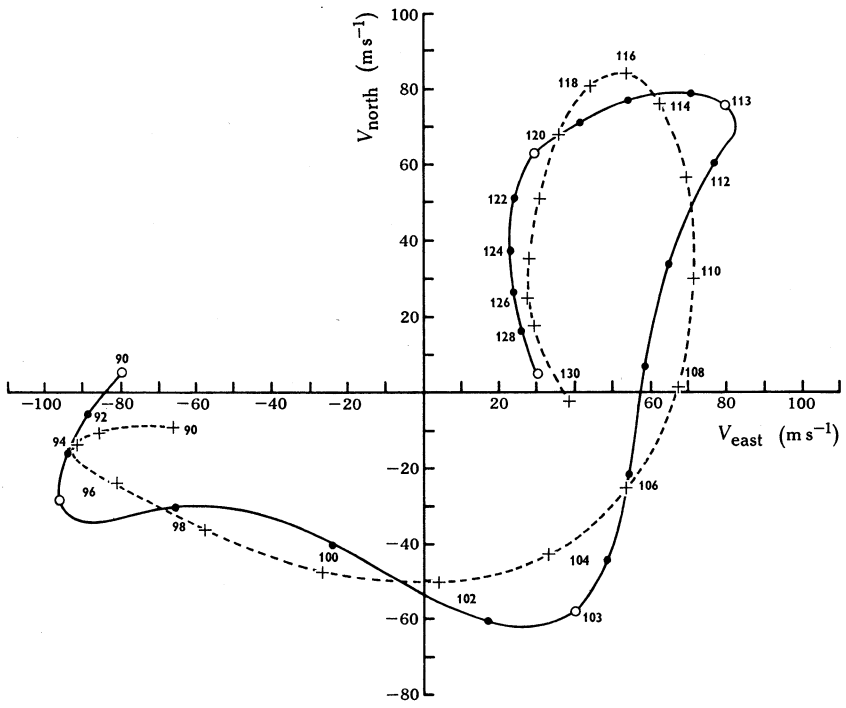

Fig. 4. Wind profile computed from the data analysis. The solid curve was derived by interpolation of the data to given times, with the open circles indicating values obtained from the identified points. The dashed curve was derived by fitting eighth-order Chebyshev polynomial expansions to the data for the northward and eastward wind profiles by means of Powell's (1964) method for error minimization. The former curve accurately reproduces the shape of the profile, while the latter provides more accurate values for the altitudes. Altitudes in km are indicated on the curves.

Although we reserve detailed discussion of the observed daytime wind profile until we have more data on daytime winds, we give here a brief description of the profile of Fig. 4. Its main characteristic is a similarity to the profiles observed at twilight and night. The spiral structure of the wind hodograph, attributed to tidal motions, proceeds anticlockwise, as would be expected in the southern hemisphere. The measured wavelength of 30 km for the spiral motion is midway between the theoretically calculated value for the dominant diurnal mode (1, 1) and semidiurnal mode (2, 4) in the upper atmosphere (20 and 40 km respectively), so that we are unable to ascribe the motion to a single mode.

Bedinger *et al.* (1968), in a discussion of the characteristics of wind profiles observed at twilight and night, have commented on the frequent appearance of 'corners' in the profile. They used the term corners to describe the manner in which the wind profile frequently consists of a series of smooth arcs, joined together in a nonsmooth manner.

The solid curve of Fig. 4, which gives the best estimate of the hodograph profile, clearly shows this characteristic. It is hoped that the nature of these corners will be solved, and that a complete description of the tidal modes will be obtained, once several lithium trails have been observed in the course of a day.

Acknowledgments

We are indebted to Mr G. Secombe, Mr W. Horne, Mr N. Talkington and Mr C. Low of the Upper Atmosphere Research Group for the suggestions they made in the inception of the instrument and for the work they did on it, both during its construction and in the field trials.

References

Bedinger, J. F. (1970). *Rev. scient. Instrum.* **41**, 1234.
Bedinger, J. F. (1973). *J. atmos. terr. Phys.* **35**, 377.
Bedinger, J. F., Knaflich, H., Manring, E., and Layzer, D. (1968). *Planet. Space Sci.* **16**, 159.
Best, G. (1970). *Appl. Optics* **9**, 266.
Hind, A. D., and Lloyd, K. H. (1973). Weapons Res. Establ. Tech. Mem. No. 1021.
Manring, E., Bedinger, J., Pettit, H., and Moore, H. (1959). *J. geophys. Res.* **64**, 587.
Murphy, C. H., and Bull, G. V. (1968). *J. geophys. Res.* **73**, 3005.
Powell, M. J. D. (1964). *Comput. J.* **7**, 155.
Rees, D., Neal, M. P., Low, C. H., Hind, A. D., Burrows, K., and Fitchew, R. S. (1972). *Nature* **240**, 32.
Rosenberg, N. W., and Golomb, D. (1963). *J. geophys. Res.* **68**, 3328.
Woodrum, A., and Justus, C. J. (1968). *J. geophys. Res.* **73**, 467.

Manuscript received 7 January 1974